tum distribution observed in the nongaussian fits signals the onset of FD quantum degeneracy, as evidenced by the good agreement between the data and the theory line presented in Fig. 5. In fact, the comparison with theory suggests that our lowest temperatures are actually closer to $T/T_F = 0.4$, consistent with our 20% systematic uncertainty in T/T_F (primarily due to uncertainty in N) (*30*).

We detected the emergence of quantum degeneracy in a trapped gas of Fermionic atoms and observed a barrier to the evaporative cooling process in a two-component Fermi gas below $0.5\ T_F$. We observed a nonclassical momentum distribution and found that the total energy of the gas is larger than the classical expectation. This excess energy is a manifestation of the Pauli exclusion principle that gives rise to an expanded momentum distribution at low T/T_F by forcing the atoms to fill higher motional states of the harmonic trapping potential. Even as T approaches zero, an ideal Fermi gas still has $\frac{3}{4}\ k_B T_F$ energy per particle; indeed, at our lowest $T/T_F \approx 0.5$ we measured an energy that is only 2.2 times this $T = 0$ limit. Reaching this quantum regime in the dilute Fermi gas extends the field of quantum degenerate gases and sets the stage for further experimental probes of a Fermi sea of atoms.

References and Notes

1. See, for example, E. P. Bashkin and A. E. Meyerovich, *J. Phys. Colloq. France* **41**, C7-61 (1980).
2. S. Inouye *et al.*, *Nature* **392**, 151 (1998); Ph. Courteille, R. S. Freeland, D. J. Heinzen, F. A. van Abeelen, B. J. Verhaar, *Phys. Rev. Lett.* **81**, 69 (1998); J. L. Roberts *et al.*, *ibid.*, p. 5109; V. Vuletic, A. J. Kerman, C. Chin, S. Chu, *ibid.* **82**, 1406 (1999).
3. For recent reviews, see E. A. Cornell, J. R. Ensher, C. E. Wieman, online abstract available at http://xxx.lanl.gov/abs/cond-mat/9903109; W. Ketterle, D. S. Durfee, D. M. Stamper-Kurn, online abstract available at http://xxx.lanl.gov/abs/cond-mat/9904034
4. J. Schneider and H. Wallis, *Phys. Rev. A* **57**, 1253 (1998); G. M. Bruun and K. Burnett, *ibid.* **58**, 2427 (1998).
5. K. Helmerson, M. Xiao, D. Pritchard, International Quantum Electronics Conference 1990, book of abstracts (IEEE, New York, 1990), abstr. QTHH4; Th. Busch, J. R. Anglin, J. I. Cirac, P. Zoller, *Europhys. Lett.* **44**, 1 (1998); J. Ruostekoski and J. Javanainen, *Phys. Rev. Lett.* **82**, 4741 (1999).
6. B. DeMarco and D. S. Jin, *Phys. Rev. A* **58**, R4267 (1998).
7. J. M. K. V. A. Koelman, H. T. C. Stoof, B. J. Verhaar, J. T. M. Walraven, *Phys. Rev. Lett.* **59**, 676 (1987).
8. G. Ferrari, *Phys. Rev. A* **59**, R4125 (1999).
9. G. Bruun and C. Clark, online abstract available at http://xxx.lanl.gov/abs/cond-mat/9905263
10. L. Vichi and S. Stringari, online abstract available at http://xxx.lanl.gov/abs/cond-mat/9905154
11. S. K. Yip and T. L. Ho, *Phys. Rev. A* **59**, 4653 (1999).
12. H. T. C. Stoof, M. Houbiers, C. A. Sackett, R. G. Hulet, *Phys. Rev. Lett.* **76**, 10 (1996); M. A. Baranov and D. S. Petrov, *Phys. Rev. A* **58**, R801 (1998); M. Houbiers and H. T. C. Stoof, *ibid.* **59**, 1556 (1999); G. Bruun, Y. Castin, R. Dum, K. Burnett, online abstract available at http://xxx.lanl.gov/abs/cond-mat/9810013.
13. B. DeMarco, H. Rohner, D. S. Jin, *Rev. Sci. Instrum.* **70**, 1967 (1999).
14. C. J. Myatt, N. R. Newbury, R. W. Ghrist, S. Loutzenhiser, C. E. Wieman, *Opt. Lett.* **21**, 290 (1996).
15. In our experiment we saw no evidence for sub-Doppler cooling processes that are used to bring some alkali gases to much colder temperatures. However, sub-Doppler cooling of ^{40}K is reported in G. Modugno, C. Benko, P. Hannaford, G. Roati, M. Inguscio, online abstract available at http://xxx.lanl.gov/abs/cond-mat/9908102
16. Y. V. Gott, M. S. Ioffe, V. G. Tel'kovski, *Nucl. Fusion* (1962 suppl.), 1045 (1962); *ibid.*, p. 1284; D. E. Pritchard, *Phys. Rev. Lett.* **51**, 1336 (1983).
17. H. F. Hess, *Phys. Rev. B* **34**, 3476 (1986); H. F. Hess *et al.*, *Phys. Rev. Lett.* **59**, 672 (1987).
18. C. J. Myatt, E. A. Burt, R. W. Ghrist, E. A. Cornell, C. E. Wieman, *Phys. Rev. Lett.* **78**, 586 (1997).
19. W. Geist, L. You, T. A. B. Kennedy, *Phys. Rev. A* **59**, 1500 (1999); E. Timmermans and R. Côté, *Phys. Rev. Lett.* **80**, 3419 (1998).
20. W. Geist, A. Idrizbegovic, M. Marinescu, T. A. B. Kennedy, L. You, online abstract available at http://xxx.lanl.gov/abs/cond-mat/9907222
21. B. DeMarco, J. L. Bohn, J. P. Burke Jr., M. Holland, D. S. Jin, *Phys. Rev. Lett.* **82**, 4208 (1999).
22. J. R. Ensher, D. S. Jin, M. R. Matthews, C. E. Wieman, E. A. Cornell, *ibid.* **77**, 4984 (1996).
23. The remaining gas was composed of 99% $m_F = 9/2$ atoms, determined from a measurement of the cross-dimensional relaxation rate (*21*).
24. D. A. Butts and D. S. Rokhsar, *Phys. Rev. A* **55**, 4346 (1997).
25. I. F. Silvera and J. T. M. Walraven, *J. Appl. Phys.* **52**, 2304 (1981); J. Oliva, *Phys. Rev. B* **39**, 4204 (1989).
26. W. Greiner, L. Neise, H. Stöcker, *Thermodynamics and Statistical Mechanics* (Springer-Verlag, New York, 1995), pp. 359–362.
27. The kinetic energy extracted from the time-of-flight absorption images equals half the total energy of the harmonically confined gas (from the equipartition theorem).
28. M. O.-Mewes *et al.*, *Phys. Rev. Lett.* **77**, 416 (1996); M. J. Holland, D. S. Jin, M. L. Chiofalo, J. Cooper, *ibid.* **78**, 3801 (1997).
29. T is obtained from the widths of the outer gaussian, σ_x and σ_z, in fits of the form given in Eq. 1. Although the effects of the FD statistics are less severe on the outer edges of the momentum distribution, these fits become less accurate as T/T_F decreases. We made a correction to T that is at most 7% based on the measured T/T_F and the results of identical fits to calculated (semiclassical) momentum distributions for an ideal Fermi gas.
30. The number of atoms N is calibrated by a florescence measurement, which has an uncertainty of $\pm 50\%$ because of intensity variations across the laser beams. The trap frequencies are determined to better than $\pm 5\%$ from center-of-mass oscillations of the trapped gas.

31. Supported by the National Institute of Standards and Technology, the NSF, and the Office of Naval Research. We thank C. Wieman, E. Cornell, and the other members of the JILA BEC group for useful discussions.

19 July 1999; accepted 16 August 1999

A Capacitance Standard Based on Counting Electrons

Mark W. Keller,[1]* Ali L. Eichenberger,[1] John M. Martinis,[1] Neil M. Zimmerman[2]

A capacitance standard based directly on the definition of capacitance was built. Single-electron tunneling devices were used to place N electrons of charge e onto a cryogenic capacitor C, and the resulting voltage change ΔV was measured. Repeated measurements of $C = Ne/\Delta V$ with this method have a relative standard deviation of 0.3×10^{-6}. This standard offers a natural basis for capacitance analogous to the Josephson effect for voltage and the quantum Hall effect for resistance.

In the past four decades, there has been an accelerating trend in metrology toward standards based on fundamental quantum properties of nature. Until 1960, all units in what is now the International System of Units (SI) were based on carefully constructed artifacts and classical physics (*1*). Quantum physics first entered the SI in 1960, when the definition of the meter was based on the wavelength of radiation from a transition in the Kr atom. A voltage standard based on the Josephson effect was first adopted in 1972 and refined in 1990, and a resistance standard based on the quantum Hall effect was adopted in 1990 (*2, 3*). For capacitance, the best existing standards are known as "calculable capacitors" and rely on a special arrangement of several electrodes such that the capacitance per unit length is related to the permittivity of free space (a defined constant in the SI) (*4*). Realizing such a standard requires precise alignment of electrodes of order 1 m in length, one of which must be movable, and compensation of end effects in order to make a system of finite length behave like an infinite system over a limited range. With the development over the past decade of single-electron tunneling (SET) devices that can precisely manipulate and detect single electrons (*5*), it is now possible to create a capacitance standard based on the quantization of electric charge (*6*). Such a standard, which we describe here, places capacitance metrology on a quantum basis and is a natural complement to the voltage and resistance standards adopted in 1990 (*7*).

Our capacitance standard combines SET devices and a low-loss cryogenic capacitor. We explain the operation of the standard, demonstrate its repeatability and uncertainty, and consider the prospects for developing our prototype into a practical calibration system. This stan-

[1]National Institute of Standards and Technology, Boulder, CO 80303, USA. [2]National Institute of Standards and Technology, Gaithersburg, MD 20899, USA.

*To whom correspondence should be addressed. E-mail: mark.keller@boulder.nist.gov

dard is the result of several years of research and development at the National Institute of Standards and Technology (NIST), and components of the standard have been described in previous publications (*8–11*).

SET devices exploit the energy required to charge a capacitance C_0 with one electron, $e^2/2C_0$. For even the smallest value of capacitance in common electronic components, 1 pF, this charging energy corresponds to a temperature of order 1 mK and is negligible in comparison to thermal fluctuations. However, modern nanolithography allows the fabrication of ultrasmall tunnel junctions with $C_0 \approx 0.1$ fF and $e^2/2C_0 \approx 10$ K. When such junctions are cooled to of order 0.1 K, SET effects completely dominate thermal fluctuations. To illustrate how SET devices allow the precise manipulation of individual electrons, we briefly explain the electron pump (*12*) shown in Fig. 1A. It consists of a chain of tunnel junctions (≈40 nm by 40 nm), with a gate capacitor coupled to the island of metal between each pair of junctions (*13*). With no voltages applied to the gate capacitors, tunneling is suppressed by the charging energy barrier. When the gates are pulsed in sequence, this barrier is selectively lowered to allow tunneling at one junction after another, and a single quantum of charge is transferred through the pump. Using our seven-junction pumps (*14*), we can routinely transfer billions of electrons with one error in every 10^8 attempts (*15*).

In defining capacitance, we consider the transfer of a charge Q between two conductors. The charge transfer creates a potential difference ΔV, and the capacitance is simply $C = Q/\Delta V$. Figure 1B shows a simple implementation of this definition based on counting electrons. Our SET capacitance standard, shown in Fig. 2A, has three critical components: (i) a seven-junction electron pump (*8, 9*), (ii) a two-junction SET transistor/electrometer (*5*) ("E" in Fig. 2A) that can detect a charge of order $e/100$ at its input capacitor, and (iii) a cryogenic vacuum-gap capacitor (*10*) having nearly ideal properties, in particular, extremely small leakage and frequency dependence. This capacitor has a three-terminal design with a well-defined value that is insensitive to stray capacitance.

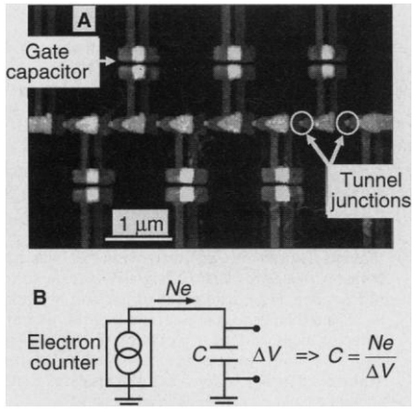

Fig. 1. (**A**) Scanning force microscope image of a seven-junction electron pump. The device consists of two layers of Al shifted horizontally by ≈0.2 μm to form tunnel junctions at the bright spots where the tip of each island overlaps its neighbor to the left. Pulsing the gates in sequence from left to right transfers electrons from left to right, and vice versa. After N cycles, the charge transferred through the pump is Ne, with an uncertainty of 1 part in 10^8. (**B**) Schematic implementation of the definition of capacitance by counting electrons.

Operation of the SET capacitance standard occurs in two phases, which we select by setting the mechanical cryogenic switches (*9*) N1 and N2. The configuration in Fig. 2A is used to determine C by counting electrons. As the pump transfers electrons, the voltage across it must be kept near zero to avoid errors. The electrometer accomplishes this by acting as a null detector for a feedback circuit that applies a voltage to the outside of C in order to keep the island between the pump and capacitor at virtual ground. This also ensures that all charge transferred through the pump appears at C and not at the 10-pF stray capacitance. After N electrons have passed through the pump, we stop the pump and measure ΔV. The configuration in Fig. 2B is used to compare C with another capacitor C_{ref} at room temperature using a conventional ac bridge. With voltages v_1 and v_2 adjusted to balance the bridge, $C/C_{ref} = v_2/v_1$.

Figure 3 shows the voltage across the capacitor as the pump transfers electrons in one direction, stops for 20 s, transfers the same number in the other direction, and repeats. We averaged the voltage data on each 20-s plateau and calculated voltage differences between successive plateaus, thus obtaining many values of ΔV for each set of data like that in Fig. 3. The average $\langle \Delta V \rangle$ determines the capacitance

$$C = Ne/\langle \Delta V \rangle \quad (1)$$

While the standard is kept at its operating temperature of 40 mK, the relative variations in the value of C are of order $1 \times 10^{-6} = 1$ part per million (ppm), as demonstrated in Fig. 4, A and B (*16*). The relative standard deviation σ for each set of data is 0.3 ppm for Fig. 4A and 0.7 ppm for Fig. 4B. The larger scatter in Fig. 4B is probably due to fluctuations in the dimensions of the vacuum-gap capacitor that did not occur during the shorter measurement period of Fig. 4A. We tested the voltage dependence of the value of C by pumping different numbers of electrons onto the capacitor, and Fig. 4C shows that there is no voltage dependence within the resolution of our measurements.

Before considering the accuracy of the SET capacitance standard, we must discuss the uncertainty (*17*) of each factor in Eq. 1. From independent tests of the pump immediately before and after operation of the standard, N has a relative uncertainty of 0.01 ppm. The uncertainties of e and $\langle \Delta V \rangle$ are subtle, and to explain them, we must briefly review the voltage standard adopted in 1990. An array of Josephson junctions excited at a frequency f produces a voltage nf/K_J, where n is an integer and $K_J = 2e/h$, where h is the Planck constant. In 1990, the following exact value was adopted by international convention: $K_{J\text{-}90} \equiv 483\,597.9$ GHz/V. This adoption of a defined value with no uncertainty established the 1990 volt, which is denoted by V_{90} and is related to the SI volt by $V_{90}/V = K_{J\text{-}90}/K_J$. The value of $K_{J\text{-}90}$ was chosen so that the 1990 volt is expected to be equivalent to the SI volt, but this equivalence has a relative uncertainty of 0.8 ppm because of uncertainties in our knowledge of various

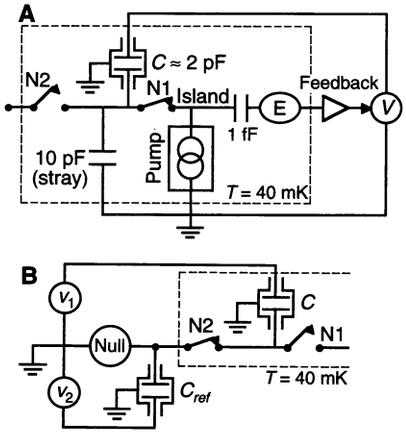

Fig. 2. Schematic diagram of the SET capacitance standard. (**A**) Configuration used to pump electrons onto C. The stray capacitance of 10 pF comes mostly from the third terminal of the vacuum-gap capacitor. (**B**) Configuration used to compare C with another capacitor at room temperature using an ac bridge.

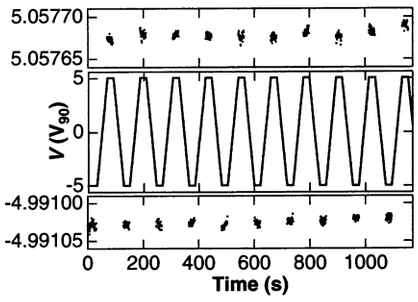

Fig. 3. Voltage applied to the capacitor by the feedback circuit while pumping electrons on and off C. Expanded views of the plateaus are shown above and below the main plot. For these data, N = 117 440 513 (= 7000001 hexadecimal) and $\langle \Delta V \rangle$ = 10.048 703 31 V_{90}, giving C = 1.872 484 77 pF from Eq. 2.

fundamental constants (*2*). We measured ΔV in terms of V_{90} (*18*), whereas for comparison with another fundamental capacitance standard we must express C in terms of the SI farad. If we naïvely use the recommended uncertainties (*19*) for the SI value of e (0.6 ppm) and for V_{90}/V (0.8 ppm), we find a combined uncertainty of $(0.6^2 + 0.8^2)^{1/2} = 1$ ppm. This implies that no matter how small the experimental uncertainty of the SET capacitance standard, the total uncertainty of C in SI units cannot be smaller than 1 ppm. However, this approach ignores the fact that the uncertainties in e and V_{90}/V are correlated. To account for this correlation, we express e in terms of the fine structure constant α and K_J as follows: $e = (4\alpha/\mu_0 c)(1/K_J)$, where $\mu_0 \equiv 4\pi \times 10^{-7}$ N/A^2 is the permeability of free space and $c \equiv 299\,792\,458$ m/s is the speed of light in vacuum (*6*). The expression for C then becomes

$$C = \frac{Ne}{\{\langle \Delta V \rangle\}_{SI} V} = \frac{N(4\alpha/\mu_0 c)(1/K_J)}{\{\langle \Delta V \rangle\}_{90} V_{90}}$$

$$= \frac{N(4\alpha/\mu_0 c)}{\{\langle \Delta V \rangle\}_{90} K_{J\text{-}90} V} \quad (2)$$

where $\{x\}_s$ denotes the dimensionless numerical value of x when it is measured in the system of units s. Because μ_0, c, and $K_{J\text{-}90}$ are defined constants, the only nonexperimental uncertainty in Eq. 2 is that of α. Currently, the recommended value (*19*) of $\alpha = 7.297\,353\,08 \times 10^{-3}$ has a relative uncertainty of 0.09 ppm, but this is expected to decrease by about a factor of 10 in the near future. Thus, the SET capacitance standard potentially offers a value of C in SI units with a total uncertainty of order 0.01 ppm if the experimental uncertainties in N and $\{\langle \Delta V \rangle\}_{90}$ can be made sufficiently small.

The accuracy of the SET capacitance standard can be tested by comparing the value of C found by counting electrons with the value measured in terms of another fundamental standard, such as a calculable capacitor. We accomplished this by using a commercial capacitance bridge (*20*) operating at 1000 Hz and calibrated with a 10-pF silica-dielectric capacitor traceable to NIST's calculable capacitor at 1592 Hz. Figure 5 shows the values of C found from counting electrons and from the bridge for the same experimental runs as Fig. 4, A and B. The uncertainty bars on the electron counting values are $\pm U_{tot} C$, where $U_{tot} = [0.09^2 + 0.01^2 + 0.1^2 + (2\sigma)^2]^{1/2}$ is the combined relative uncertainty (in parts per million) from α, N, the voltmeter itself, and the statistical variations in each set of data. The uncertainty bars on the bridge values are ± 2.4 ppm owing to the uncertainty in the value of the 10-pF capacitor at 1000 Hz. Within these uncertainties, the measurement from counting electrons agrees with the measurement traceable to a calculable capacitor. We think that the actual systematic errors in the SET capacitance standard are smaller than the upper bound of ≈ 2 ppm demonstrated here, and we are pursuing a better comparison with a calculable capacitor.

The performance of our prototype is already impressive enough to suggest that a capacitance standard based on counting electrons will play an important role in electrical metrology. However, there are several issues that must be addressed before the SET capacitance standard can fulfill this promise (*11*). We briefly mention three important issues here, with further details to be presented elsewhere. (i) The frequency dependence of the cryogenic capacitor must be very small because the measurement of C by counting electrons occurs at an effective frequency much lower than that used for bridge comparisons. (ii) The input noise of the electrometer limits the ability of the feedback circuit to maintain virtual ground between the pump and the capacitor. Reducing this noise, which has a $1/f$ power spectrum and is caused by moving charged defects within or near the electrometer, will be important in achieving the full potential of the standard. (iii) A thorough analysis of the circuits in Fig. 2 must be performed to determine the magnitudes of all possible uncertainties in both phases of operation.

The SET capacitance standard described here makes it possible to place capacitance metrology on a quantum basis, as was done previously for voltage and resistance. For this new standard to become a practical tool for metrologists, it must be developed into a system that is robust and easy to use, with a total relative uncertainty of order 0.1 ppm. Although the engineering challenges involved are substantial, our present understanding of the requirements for reliable operation of SET devices indicates that they can be met. We hope that ultimately the SET capacitance standard will join the Josephson voltage standard and the quantum Hall resistance standard as a widely adopted natural standard for electrical metrology.

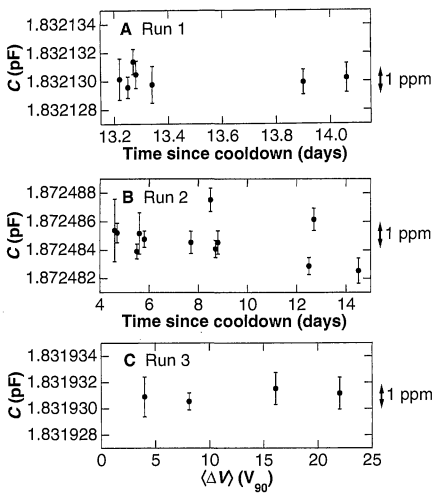

Fig. 4. Repeatability of the SET capacitance standard with $\langle \Delta V \rangle \approx 10$ V during periods of (**A**) 24 hours and (**B**) 10 days. (**C**) Measurements of C over a range of $\langle \Delta V \rangle$ show that the standard is independent of voltage. Uncertainty bars are ± 1 SD from the mean within each measurement.

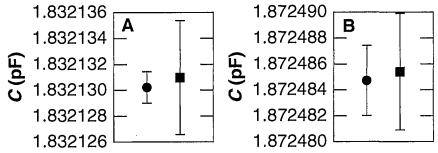

Fig. 5. Comparison of C from counting electrons (solid circles) and from a commercial ac bridge that is traceable to a calculable capacitor (solid squares). The electron counting values in (**A**) and (**B**) are the averages of the data in the corresponding parts of Fig. 4 and the bridge measurements were taken during the same conditions. Uncertainty bars are $\pm U_{tot} C$ for the electron counting values and ± 2.4 ppm for the bridge values.

References and Notes

1. B. N. Taylor, Ed., *The International System of Units (SI)*, *NIST Spec. Publ. 330* (Government Printing Office, Washington, DC, 1991) (available at http://physics.nist.gov/Document/sp330.pdf).
2. B. N. Taylor and T. J. Witt, *Metrologia* **26**, 47 (1989).
3. The 1990 volt and ohm have not been formally integrated into the SI, but they are in use worldwide as practical units because they can be reproduced with much smaller uncertainty than the SI volt and ohm.
4. W. K. Clothier, *Metrologia* **1**, 36 (1965).
5. H. Grabert and M. H. Devoret, Eds., *Single Charge Tunneling* (Plenum, New York, 1992).
6. E. R. Williams, R. N. Ghosh, J. M. Martinis, *J. Res. Natl. Inst. Stand. Technol.* **97**, 299 (1992).
7. N. M. Zimmerman, *Am. J. Phys.* **66**, 324 (1998).
8. M. W. Keller, J. M. Martinis, N. M. Zimmerman, A. H. Steinbach, *Appl. Phys. Lett.* **69**, 1804 (1996).
9. M. W. Keller, J. M. Martinis, A. H. Steinbach, N. M. Zimmerman, *IEEE Trans. Instrum. Meas.* **46**, 307 (1997).
10. N. M. Zimmerman, *ibid.* **45**, 841 (1996).
11. ———, J. L. Cobb, A. F. Clark, *ibid.* **46**, 294 (1997).
12. H. Pothier, P. Lafarge, C. Urbina, D. Esteve, M. H. Devoret, *Europhys. Lett.* **17**, 249 (1992).
13. We fabricated these structures by evaporating Al through a suspended polymer mask that was patterned with electron beam lithography. We deposited Al from one angle, oxidized it to form an insulating layer, and then deposited a second layer of Al from a different angle so that it partially overlaps the first layer. This forms metal-insulator-metal sandwiches in the overlapping regions, and the insulator is thin enough to allow quantum tunneling.
14. Although an electron pump can be made with as few as three junctions, we used seven junctions in order to suppress undesired multijunction tunneling events that are rare but not negligible at temperatures well below the charging energy barrier.
15. We focus here on electron counting, but the pump is also an accurate current source. The maximum current of ≈ 10 pA is too small for conventional metrology, but it can be useful in situations where accurate measurements of extremely small currents are needed.
16. Thermal cycling to room temperature between these two experimental runs caused C to change by $\approx 2\%$ because of mechanical changes in the capacitor. Un-

like an artifact, the SET standard is not affected by this change because C is determined in situ each time the standard is cooled and operated.
17. Throughout this report, we use expanded uncertainty with coverage factor $k = 2$, which defines an interval that is expected to contain ≈95% of the reasonable values for the measured quantity.
18. We used a digital voltmeter that was calibrated with a Josephson voltage standard and has a relative uncertainty of 0.1 ppm for its range of 10 V. The finite input current of the voltmeter is supplied by the feedback circuit and does not affect the measurement of ΔV.
19. E. R. Cohen and B. N. Taylor, *Rev. Mod. Phys.* **57**, 1121 (1987).
20. We used commercial capacitance bridge model AH2500A (Andeen-Hagerling, Cleveland, OH). The identification of specific commercial instruments does not imply endorsement by NIST nor does it imply that the instruments identified are the best available for a particular purpose.
21. The authors gratefully acknowledge voltage calibration assistance from C. Hamilton, capacitance calibration assistance from A.-M. Jeffery, and discussions with E. Williams regarding Eq. 2.

19 May 1999; accepted 29 July 1999

Increased Summertime UV Radiation in New Zealand in Response to Ozone Loss

Richard McKenzie,* Brian Connor, Greg Bodeker

Long-term decreases in summertime ozone over Lauder, New Zealand (45°S), are shown to have led to substantial increases in peak ultraviolet (UV) radiation intensities. In the summer of 1998–99, the peak sunburning UV radiation was about 12 percent more than in the first years of the decade. Larger increases were seen for DNA-damaging UV radiation and plant-damaging UV radiation, whereas UV-A (315 to 400 nanometers) radiation, which is insensitive to ozone, showed no increase, in agreement with model calculations. These results provide strong evidence of human-induced increases in UV radiation, in a region where baseline levels of UV radiation were already relatively high.

Ozone depletion, caused by the buildup of man-made chemicals in the atmosphere, is a concern because it leads to increased UV radiation at Earth's surface. Even relatively small increases in UV radiation can have serious impacts on human health, the biosphere, and materials. For example, a reduction in ozone of 1% leads to increases of up to 3% in some forms of nonmelanoma skin cancers (*1*). However, although the inverse relation between ozone and UV radiation is well established (*2*, *3*), the determination of trends from UV radiation measurements has been more problematic than for ozone. First, UV radiation measurements generally have a lower precision because they require an absolute calibration rather than the simpler relative calibration required for ozone determination. Second, UV radiation is more variable because it is strongly influenced by several factors other than ozone: notably solar zenith angle (sza), volcanic impacts, tropospheric aerosols, cloud cover, and surface albedo. These factors have compromised the ability of previous studies to unequivocally attribute increases in UV radiation to long-term declines in ozone (*2*, *3*). Here, we report a close correspondence between UV radiation changes calculated from ozone data and measured UV irradiances from Lauder, New Zealand.

Research into atmospheric ozone and its effects on UV radiation is undertaken by the National Institute of Water and Atmospheric Research (NIWA) at its laboratory in Lauder (45.04°S, 169.68°E, 370 m), Central Otago, New Zealand. This research has confirmed the expected downward trend in ozone associated with the buildup of ozone-depleting chemicals in the atmosphere. For annually averaged ozone, the largest decreases at this site occurred in the mid-1980s (*4*). Summertime ozone shows a more monotonic decrease with time (Fig. 1A). In recent years, it has been about 10 to 15% less than in the 1970s, before man-induced ozone depletion first became apparent. Superimposed on this downward trend are shorter term variabilities due to dynamical effects associated with changes in tropopause height, volcanic eruptions, the Quasi-Biennial Oscillation, the El Niño–Southern Oscillation, and the 11-year solar cycle. At this site, unlike other latitudes, the eruption of Mount Pinatubo (1991) had only a minor influence on ozone or peak global UV irradiance (*4*, *5*).

From the viewpoint of UV radiation and its effects on the biosphere, changes in ozone during the summer are particularly important, because at midlatitudes, the annual UV radiation dose is dominated by that received in the summer months. At Lauder, midday doses of erythemally weighted (*6*, *7*) (or "sunburning") UV radiation in winter are only 10% of those in the summer, and wintertime daily integrals are only 6% of summer values because of reduced daylight hours (*8*).

The UV radiation in the south has historically been more intense because of hemispheric differences in ozone and because the closest Earth-sun separation occurs during the Southern Hemisphere summer. Model calculations of erythemal UV radiation for clear-sky summer conditions are ~10 to 15% more for southern midlatitudes than for the north (*1*, *9*). Measurements that directly compare UV radiation in New Zealand with that in Europe have shown much larger differences (*10*, *11*). Even in the 1970s, before substantial ozone depletion had occurred, erythemal UV radiation at 45°S was probably substantially greater than during the 1990s at 45°N (*1*). In addition, in the Southern Hemisphere, ozone depletion has occurred all year round, whereas in the Northern Hemisphere, the depletions have been less severe in the summer (*3*). The resultant relatively intense UV radiation may be a factor contributing to the high rates of skin cancer in New Zealand (*12*), although other factors such as lifestyle and skin type are also important.

The changes in the UV radiation that would be expected from the changes in ozone observed at Lauder are shown in Fig. 1B, where the results are expressed in terms of the noontime UV Index, a standardized way of reporting UV radiation to the public (*13*). This UV Index was calculated with a sensitivity factor (RAF) of erythemal UV radiation to ozone change (*14*) and normalized to match measured values at the middle of the period for which measurements were available. The calculated UV Index increases with time in anticorrelation with the changes in ozone and in the summer of 1998–99 was the highest to date, about 15 to 20% higher than in the late 1970s.

Here we demonstrate a close correspondence between these calculated changes and those derived from spectral measurements of UV global irradiances obtained at Lauder since December 1989. The spectra were taken at 5° steps in sza and at 15-min intervals for a 90-min period centered at midday. The accuracy of biologically weighted integrals derived from these spectra for trend determination is limited mainly by the repeatability of the calibrations, which are estimated to be better than ±3% (*15*).

To minimize the effects of factors other than ozone, we considered a subset of the UV radiation data. First, we took the mean UV Index each day from the five spectra measured at 15-min intervals over a 1-hour period centered at local solar noon. By selecting

National Institute of Water and Atmospheric Research, NIWA Lauder, PB 50061 Omakau, Central Otago, New Zealand.

*To whom correspondence should be addressed. E-mail: r.mckenzie@niwa.cri.nz